arXiv:1605.06797v1 [cond-mat.mtrl-sci] 22 May 2016

Low Gilbert damping in Co_2FeSi and Fe_2CoSi films

Christian Sterwerf,[1,*] Soumalya Paul,[2] Behrouz Khodadadi,[2] Markus Meinert,[1]
Jan-Michael Schmalhorst,[1] Mathias Buchmeier,[2] Claudia K. A. Mewes,[2] Tim Mewes,[2] and Günter Reiss[1]

[1] *Center for Spinelectronic Materials and Devices, Physics Department, Bielefeld University, Germany*
[2] *Department of Physics and Astronomy/MINT Center, The University of Alabama, Tuscaloosa, AL 35487, USA*

(Dated: May 24, 2016)

Thin highly textured $Fe_{1+x}Co_{2-x}Si$ ($0 \leq x \leq 1$) films were prepared on MgO (001) substrates by magnetron co-sputtering. The magneto-optic Kerr effect (MOKE) and ferromagnetic resonance (FMR) measurements were used to investigate the composition dependence of the magnetization, the magnetic anisotropy, the gyromagnetic ratio and the relaxation of the films. The effective magnetization for the thin $Fe_{1+x}Co_{2-x}Si$ films, determined by FMR measurements, are consistent with the Slater Pauling prediction. Both MOKE and FMR measurements reveal a pronounced fourfold anisotropy distribution for all films. In addition we found a strong influence of the stoichiometry on the anisotropy as the cubic anisotropy strongly increases with increasing Fe concentration. The gyromagnetic ratio is only weakly dependent on the composition. We find low Gilbert damping parameters for all films with values down to 0.0012 ± 0.00012 for $Fe_{1.75}Co_{1.25}Si$. The effective damping parameter for Co_2FeSi is found to be 0.0018 ± 0.0004. We also find a pronounced anisotropic relaxation, which indicates significant contributions of two-magnon scattering processes that is strongest along the easy axes of the films. This makes thin $Fe_{1+x}Co_{2-x}Si$ films ideal materials for the application in STT-MRAM devices.

I. INTRODUCTION

Half-metallic ferromagnets have attracted great interest during the past few years because they promise to boost the performance of spintronic devices. High spin polarization at the Fermi level can generate high tunnel magnetoresistance (TMR) ratios. A TMR effect can be measured in a magnetic tunnel junction (MTJ) that consists of two ferromagnetic films separated by a thin insulator. The same structures can also be utilized to spin transfer torque induced magnetization switching [1], however in this case a low switching current density is desirable. Thus, low magnetic damping and a high spin polarization are frequently required for spin transfer torque based devices [2]. A high spin polarization can be found in half-metals where one spin band structure is semiconducting while the other spin band structure is metallic. Co- and Fe-based Heusler compounds are good candidates for materials with high Curie temperatures and half-metallic behavior.

Full Heusler compounds have the formula X_2YZ, where X and Y are transition metals and Z is a main group element. There are two different ordered structures: the $L2_1$ structure and the X_a structure with a different occupation sequence. Both structures consist of a four-atom basis and an fcc lattice. The prototype of the $L2_1$ structure is Cu_2MnAl (space group $Fm\bar{3}m$) with the occupation sequence X-Y-X-Z [3]. The prototypes for the X_a structure are Hg_2CuTi and Li_2AgSb with an occupation sequence Y-X-X-Z, with the two X-atoms at inequivalent positions in the lattice [4, 5]. In this work, we investigate the magnetic properties of a stoichiometric series ranging from Co_2FeSi to Fe_2CoSi, where Co_2FeSi crystalizes in the $L2_1$ structure and Fe_2CoSi in the X_a structure, respectively. Both compounds should have a (pseudo-)gap in the minority states as predicted by first principle calculations. By substituting Co and Fe atoms the number of electrons varies and the Fermi level is expected to be shifted to lower energies when the Fe concentration is increased. As we reported previously, magnetic tunnel junctions based on the $Fe_{1+x}Co_{2-x}Si$ films exhibit very high TMR ratios for all stoichiometries [6]. At 15 K a maximum TMR ratio of 262% was found for the intermediate stoichiometry $Fe_{1.75}Co_{1.25}Si$, while the Co_2FeSi and Fe_2CoSi based MTJs showed a TMR ratio of 167% and 227%, respectively. One possible explanation for the high TMR ratio is that for $Fe_{1.75}Co_{1.25}Si$ the Fermi energy is shifted inside the pseudo-gap. In this work we present results of the magnetic properties for the magnetization dynamics in particular including anisotropy and the Gilbert damping parameter of the $Fe_{1+x}Co_{2-x}Si$ films, as the intrinsic relaxation is are expected to be low for half-metals [7].

II. PREPARATION AND CHARACTERIZATION TECHNIQUES

Thin $Fe_{1+x}Co_{2-x}Si$ (x=0, 0.25, 0.5, 0.75, 1) films were fabricated using co-sputtering in an UHV sputtering system with a base pressure of $1 \cdot 10^{-9}$ mbar. The Ar pressure during sputtering was $2 \cdot 10^{-3}$ mbar. The films were grown by dc- and rf-magnetron sputtering from elemental targets onto MgO (001) substrates. Additional MgO and Cr seed layers were used to accommodate small lattice mis-

* csterwerf@physik.uni-bielefeld.de

matches and to promote coherent and epitaxial growth, as the Cr seed layer grows in 45° direction on the MgO layer, which has a lattice parameter of 4.212 Å. The lattice mismatch between two unit cells of Cr (2×2.885 Å at 20°C [8]) and one unit cell of Co_2FeSi (5.64 Å [9]) or Fe_2CoSi (5.645 Å [10]) is about 2%. The 5 nm thick MgO and Cr films were in-situ annealed at 700°C to obtain smooth surfaces. $Fe_{1+x}Co_{2-x}Si$ films with a thickness of 20 nm were deposited at room temperature and ex-situ vacuum annealed at 500°C. A 2 nm thick MgO capping layer was used to prevent oxidation of the films. To determine the stoichiometry and to adjust the sputtering powers, x-ray fluorescence measurements were carried out. To obtain information about the magnetization dynamics, in-plane ferromagnetic resonance (FMR) measurements were performed using a broadband coplanar waveguide setup up to a maximum frequency of 40 GHz. Least square fits of the raw data using a first derivative of a Lorenzian line shape were done to precisely determine the resonance field and the peak-to-peak linewidth ΔH [11, 12]. For the FMR in-plane angle dependent measurements the samples were mounted on a rotating stage and the resonance spectra were measured at a frequency of 30 GHz while the in-plane angle was changed in 5° steps. In addition quasistatic magnetization reversal measurements were carried out using the magneto-optic Kerr effect (MOKE) in a vector MOKE setup with an s-polarized laser with a wavelength of 488 nm. Anisotropy measurements were carried out using a rotating sample holder. The magnetic field was applied in the plane of the films.

III. CRYSTALLOGRAPHIC PROPERTIES

X-ray diffraction measurements were used to investigate the crystallographic properties of the $Fe_{1+x}Co_{2-x}Si$ films. Ordering parameters, determined from x-ray diffraction, were already discussed in our previous work [6] and found to be high for Co_2FeSi and decrease when going to Fe_2CoSi. In order to test the films for crystallographic symmetry φ scans are performed on the (220) planes of the $Fe_{1+x}Co_{2-x}Si$ films. Figure 1 shows the results together with the (220) plane of the MgO (001) substrate. The result shows that the (100) Heusler plane is rotated by 45° with respect to the MgO (100) plane. The fourfold symmetry of the φ-scans clearly verifies the highly textured growth of all $Fe_{1+x}Co_{2-x}Si$ films of this study.

IV. MAGNETIZATION DYNAMICS

In this section we present in-plane broadband FMR measurements for the $Fe_{1+x}Co_{2-x}Si$ samples to obtain information about the magnetic properties of the films. The Landau-Lifshitz-Gilbert equation describes the dynamics of the magnetization vector $\vec{M}$ in the presence

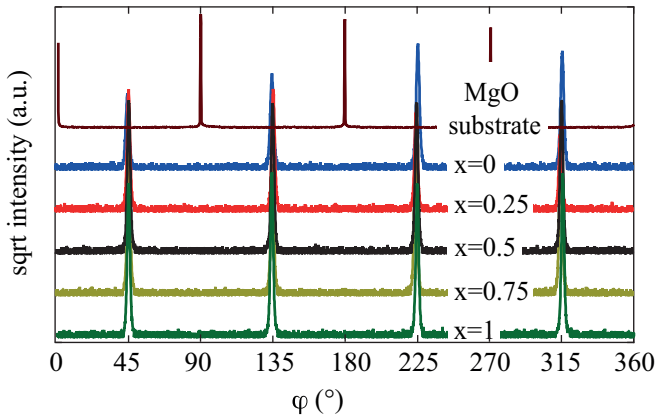

FIG. 1. φ-scans of the (220) $Fe_{1+x}Co_{2-x}Si$ peak and (220) MgO substrate peak showing the fourfold symmetry of the films.

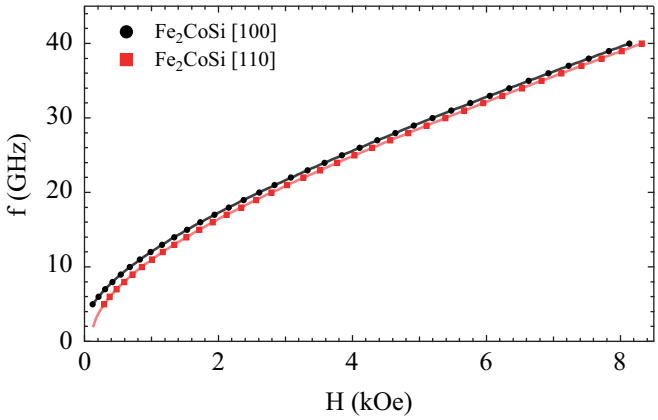

FIG. 2. Resonance frequency versus magnetic field (Kittel plot) along the in-plane magnetic hard [110] and the magnetic easy [100] axis for Fe_2CoSi. The experimental data are fitted using a combined fit (equations (3 and 4)) to determine M_{eff} and γ'.

of an effective field $\vec{H}_{\text{eff}}$, which contains both dc and ac fields.

It is given by [13]:

$$\frac{\mathrm{d}\vec{M}}{\mathrm{d}t} = -\gamma \vec{M} \times \vec{H}_{\text{eff}} + \frac{\alpha}{M}\left(\vec{M} \times \frac{\mathrm{d}\vec{M}}{\mathrm{d}t}\right), \qquad (1)$$

where γ is the gyromagnetic ratio and the quantity parameter α is the Gilbert damping parameter. According to the Landau-Lifshitz-Gilbert equation (1), the resonance condition can be expressed in terms of the second derivatives of the free-energy density E by the Smit-Beljers formula [14]:

$$\left(\frac{f}{\gamma'}\right)^2 = \frac{1}{(M\sin\theta)^2}\left[\frac{\partial^2 E}{\partial\theta^2}\frac{\partial^2 E}{\partial\varphi^2} - \left(\frac{\partial^2 E}{\partial\theta\partial\varphi}\right)^2\right]\Bigg|_{\theta_0,\varphi_0} \qquad (2)$$

where $\gamma' = \gamma/2\pi$, θ and φ are the polar and azimuthal angles of the magnetization $\vec{M}$ and θ_0 and φ_0 the corre-

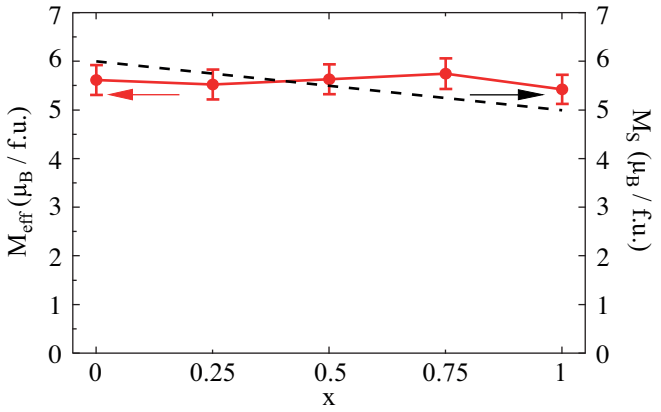

FIG. 3. Dependence of the fitted effective magnetic moment per formula unit for $Fe_{1+x}Co_{2-x}Si$ films with x=0, 0.25, 0.5, 0.75, 1 shown on the left axis. The dashed line shows the interpolated expected magnetic moments according to the Slater-Pauling rule (right axis).

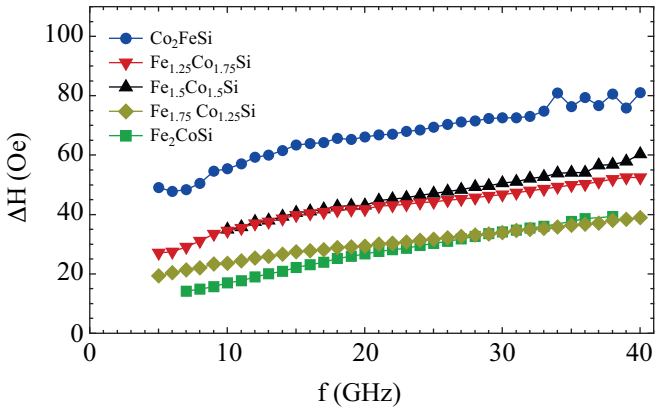

FIG. 4. Frequency dependent FMR linewidth for all samples measured along the magnetic hard axis [110] of the $Fe_{1+x}Co_{2-x}Si$ films.

sponding equilibrium values. Measurements of the magnetic field dependent resonance frequency were carried out in two different orientations of the sample: in [100] and [110] direction of the $Fe_{1+x}Co_{2-x}Si$ Heusler alloy, as the [100] direction is the magnetic easy axis and the [110] direction the magnetic hard axis, respectively. Figure 2 shows the exemplary Kittel plots along [100] and [110] directions for the Fe_2CoSi sample. The experimental data were fitted simultaneously using the Kittel equation for both easy and hard configurations [15]:

$$f = \gamma' \sqrt{(H_{\mathrm{res-ha}} - H_4)(H_{\mathrm{res-ha}} + \frac{H_4}{2} + 4\pi M_{\mathrm{eff}})} \quad (3)$$

$$f = \gamma' \sqrt{(H_{\mathrm{res-ea}} + H_4)(H_{\mathrm{res-ea}} + H_4 + 4\pi M_{\mathrm{eff}})} \quad (4)$$

where M_{eff}, γ' and H_4 are shared fit parameters. H_4 describes the magnitude of the in-plane fourfold anisotropy field. $H_{\mathrm{res-ha}}$ and $H_{\mathrm{res-ea}}$ denote the resonance field along the magnetic hard and the magnetic easy axis, respectively. The resulting fit parameters for the gyromagnetic ratio γ' are presented in Fig. 6 a) for all x in $Fe_{1+x}Co_{2-x}Si$. Within the error bars it is nearly constant for x $\geq$ 0.25 and slightly smaller for Co_2FeSi. The fitted effective magnetization, which includes any perpendicular anisotropy present in the films, is shown in Fig. 3 for the $Fe_{1+x}Co_{2-x}Si$ samples. The error bars originate from fitting of the Kittel equations and the determination of the volume of the unit cell. For bulk Co_2FeSi and Fe_2CoSi the experimentally determined magnetizations are 5.95 μ_B/f.u.[9] and 4.99 μ_B/f.u.[10], respectively, which match the expected magnetizations according to the Slater-Pauling rule (visualized by the dashed line in Fig. 3 on the right axis). The deviation from the expected values might be attributed to residual atomic disorder in the films or the presence of a perpendicular anisotropy caused by a small tetragonal distortion in the [001] direction.

The frequency dependence of the linewidth of the ferromagnetic resonance absorption provides direct information about the magnetic relaxation. The frequency dependence of the linewidth [16, 17] can under certain conditions be characterized by an inhomogeneous residual linewidth at zero field ΔH_0 and an intrinsic contribution [18]:

$$\Delta H = \Delta H_0 + \frac{2}{\sqrt{3}} \frac{\alpha_{\mathrm{eff}}}{\gamma'} f. \quad (5)$$

For correct determination of the effective damping parameter it is necessary to measure the linewidth over a wide frequency range to determine the slope. It is not sufficient to measure ΔH at a fixed frequency, because a non-zero extrinsic linewidth ΔH_0 results in an overestimated damping parameter α_{eff}. Figure 4 shows the peak-to-peak linewidth ΔH for all frequencies and all x. The measurements were performed in the direction of the magnetic hard axis of the Heusler films. The experimental data were fitted by equation (5) to determine the effective damping parameters. The slope at higher frequencies was used to determine the damping parameters. The inhomogeneous residual linewidth at zero field ΔH_0 is presented in Fig. 6 b) for all stoichiometries. The error margins result from the different slopes in the ΔH vs. f curves. The residual linewidth decreases as the Fe concentration increases and reaches its lowest value of $\Delta H_0 = 12$ Oe for Fe_2CoSi. McMichael *et al.* [19] found that small grain size distributions can lead to low inhomogeneous line broadening.

The effective Gilbert damping parameter α_{eff} is shown in Fig. 6 c). All damping parameters have the same order of magnitude and vary between 0.0012 ± 0.00012 to 0.0019 ± 0.00013. The very upper limit of the error margins was calculated assuming that the linewidth measured at 40 GHz is caused solely by Gilbert type damping. Co_2FeSi exhibits a damping parameter of 0.0018 ± 0.0004, while Fe_2CoSi shows a slightly larger value of 0.0019 ± 0.00013. Kasatani *et al.* found damping

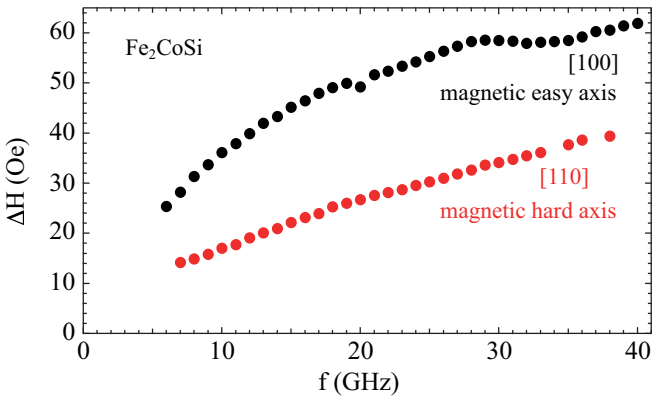

FIG. 5. FMR linewidth for Fe_2CoSi measured along both the magnetic hard [110] and magnetic easy [100] axis.

parameters from 0.0023 to 0.0061 for Co_2FeSi films and 0.002 for Fe_2CoSi [20]. In general, the Gilbert damping is expected to be low in half-metallic materials, where spin-flip processes are suppressed [7, 21]. The small damping parameters of the metallic films show that a pseudo-gap as present in the $Fe_{1+x}Co_{2-x}Si$ system is sufficient to give rise to a low Gilbert damping.

Figure 5 shows the frequency dependent linewidth along easy and hard axes for the Fe_2CoSi. The linewidth exhibits almost linear behavior (the Gilbert model) along the hard axis. We observed non-linear behavior in the linewidth vs. frequency response along the magnetic easy axis. This nonlinear dependence of the FMR linewidth on frequency is a typical observation when two magnon scattering contributes significantly to the relaxation [22, 23]. Two-magnon scattering is an extrinsic relaxation mechanism and can be induced by means of different scattering centers such as voids or pores [24], surface roughness [22] and grain size [25] or by network of misfit dislocations which causes scattering of the FMR mode (k=0) into propagating spin waves (k≠0).

A. FMR in-plane rotation measurements

To obtain further information about the magnetic anisotropies and magnetic relaxation additional FMR measurements were carried out as a function of the in-plane angle of the applied field with respect to the $Fe_{1+x}Co_{2-x}Si$ [110] axis. The operating frequency for the rotation measurements was 30 GHz. At this frequency the resonance fields are high enough to saturate the magnetization along the easy and hard axes. All measurements were performed at room temperature.

A fourfold symmetry is observed in the in-plane angle dependence of the ferromagnetic resonance field for all samples. Figure 7 a) exemplarily shows the ferromagnetic resonance field H_{res} versus the in-plane rotation angle for Fe_2CoSi. The dependence of the resonance field on the in-plane angle was simulated numerically using equation

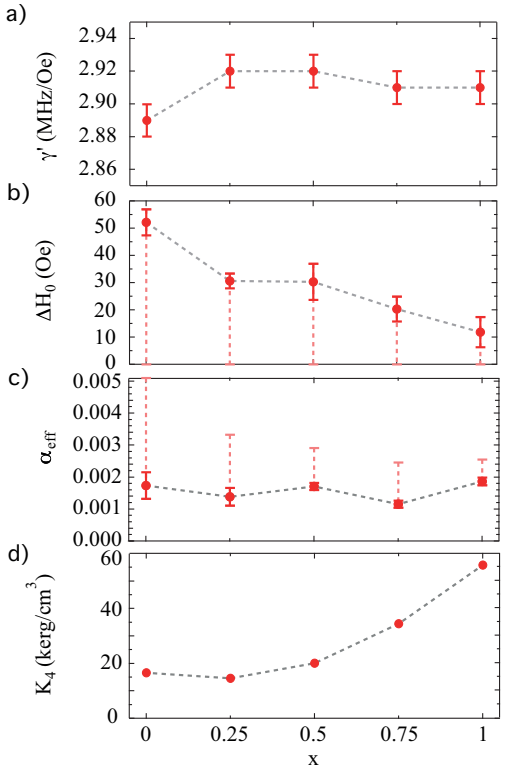

FIG. 6. a) Gyromagnetic ratio γ', b) Extrinsic contribution to the linewidth ΔH_0 of the FMR spectra, c) effective Gilbert damping parameter and d) cubic magnetic anisotropy constant K_4 for $Fe_{1+x}Co_{2-x}Si$ films with $x = 0,\ 0.25,\ 0.5,\ 0.75$,1.

(2), assuming a cubic magnetic anisotropy contribution to the Gibbs free energy [26, 27]:

$$E_{\text{cubic}} = -\frac{1}{2}K_4\left(\alpha_1^4 + \alpha_2^4 + \alpha_3^4\right), \qquad (6)$$

where K_4 is the cubic magnetic anisotropy constant and α_1, α_2, α_3 are the directional cosines with respect to the cubic principal axes. The experimentally determined in-plane angle dependent H_{res} data were fitted with the numerical solution (red line in Fig. 7 a)) to determine the cubic anisotropy constant. Figure 7 b) shows the corresponding linewidth data, which also shows a clear fourfold symmetry. The linewidth exhibits maxima along the easy axes and minima along the hard axes of the cubic magnetic anisotropy. Randomly distributed crystalline defects oriented along the in-plane principal crystallographic axis [28] or a fourfold distribution in misfit dislocations [29] which induce the same symmetry on the strength of two magnon scattering can explain the observed anisotropic relaxation.

The magnetic fourfold symmetry matches the crystallographic symmetry of the highly textured $Fe_{1+x}Co_{2-x}Si$ films mentioned before. A polar plot of the MOKE squareness versus the rotational angle for Fe_2CoSi is presented in Fig. 8. This measurement confirms the cubic

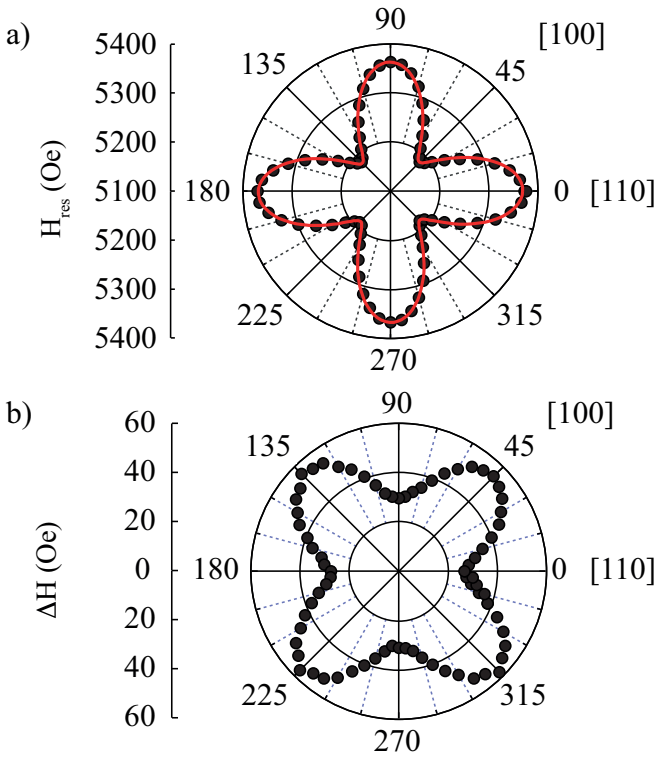

FIG. 7. Polar plots of a) the resonance fields H_{res} and b) the linewidth ΔH as a function of the in-plane angle of the applied field with respect to the [110] axis of a 20 nm thick Fe_2CoSi film measured at a microwave frequency of 30 GHz.

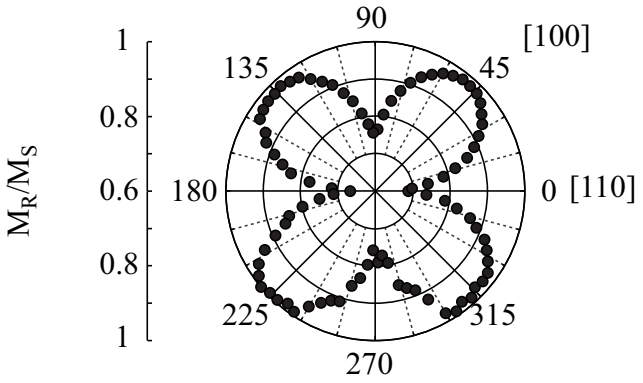

FIG. 8. Polar plots of the squareness $\frac{M_R}{M_S}$ for Fe_2CoSi obtained by MOKE measurements.

anisotropy present in the films as seen in the FMR measurement. The magnetic easy axis is located along the [100] crystallographic axis and the magnetic hard axis is located along the [110] crystallographic axis. A cubic anisotropy with the easy magnetic axis in the Heusler [100] direction is found for all samples. The cubic magnetic anisotropy constant K_4 obtained from the FMR measurements changes significantly in this series from $55.8\,\frac{\text{kerg}}{\text{cm}^3}$ for Fe_2CoSi to $16.6\,\frac{\text{kerg}}{\text{cm}^3}$ for Co_2FeSi, respectively. The cubic anisotropy constants for all stoichiometries are presented in Fig. 6 d). Hashimoto *et al.* found a similar cubic anisotropy constant of $18\,\frac{\text{kerg}}{\text{cm}^3}$ for crystalline Co_2FeSi with a film thickness of 18.5 nm [30]. Some films show an additional uniaxial anisotropy component, which can originate from miscut substrates.

V. CONCLUSION

In summary we found very small damping parameters for the half-metallic $Fe_{1+x}Co_{2-x}Si$ films varying from 0.0012 ± 0.00012 to 0.0019 ± 0.00013. Co_2FeSi exhibits a damping parameter of 0.0018 ± 0.0004. Thus, the films are suitable for the use in STT-MRAMs. FMR and MOKE measurements reveal a fourfold magnetocrystalline anisotropy for all films in accordance with the fourfold crystalline symmetry in the highly textured films. The need for frequency dependent FMR measurements was exemplified by the finding that the residual linewidth changes both with composition and with the measurement direction.

ACKNOWLEDGMENTS

The authors gratefully acknowledge financial support from Bundesministerium für Bildung und Forschung (BMBF) and Deutsche Forschungsgemeinschaft (DFG, contract no. RE 1052/32-1) as well as support through the MINT Center summer program. S. Paul, B. Khodadadi and T. Mewes would like to acknowledge support by the NSF-CAREER Award No. 0952929, C.K.A. Mewes would like to acknowledge support by the NSF-CAREER Award No. 1452670.

[1] L. Berger, Physical Review B **54**, 9353 (1996).
[2] J. C. Slonczewski, Journal of Magnetism and Magnetic Materials **159**, L1 (1996).
[3] A. J. Bradley and J. W. Rodgers, Proceedings of the Royal Society of London Series A **144**, 340 (1934).
[4] M. Puselj and Z. Ban, Croat. Chem. Acta **41**, 79 (1969).
[5] H. Pauly, A. Weiss, and H. Witte, Z. Metallkunde **59**, 47 (1968).
[6] C. Sterwerf, M. Meinert, J.-M. Schmalhorst, and G. Reiss, IEEE Transactions on Magnetics **49**, 4386 (2013).
[7] C. Liu, C. Mewes, M. Chshiev, and T. Mewes, Applied Physics Letters **95**, 022509 (2009).
[8] M. E. Straumanis and C. C. Weng, Acta Crystallographica **8**, 367 (1955).
[9] S. Wurmehl, G. Fecher, H. Kandpal, V. Ksenofontov, C. Felser, H.-J. Lin, and J. Morais, Physical Review B **72**, 184434 (2005).
[10] H. Luo, Z. Zhu, L. Ma, S. Xu, H. Liu, J. Qu, Y. Li, and G. Wu, Journal of Physics D: Applied Physics **40**, 7121 (2007).
[11] M. E. Schabes, H. Zhou, and H. N. Bertram, Journal of Applied Physics **87**, 5666 (2000).
[12] N. Pachauri, B. Khodadadi, and M. Althammer, Journal of Applied Physics **117**, 233907 (2015).
[13] B. Heinrich and J. F. Cochran, Advances in Physics **42**, 523 (1993).
[14] H. Suhl, Physical Review **97**, 555 (1955).
[15] X. Liu, Y. Sasaki, and J. K. Furdyna, Physical Review B **67**, 205204 (2003).
[16] B. Heinrich, J. F. Cochran, and R. Hasegawa, Journal of Applied Physics **57**, 3690 (1985).
[17] H. Lee, L. Wen, M. Pathak, and P. Janssen, Journal of Physics D: Applied Physics **41**, 215001 (2008).
[18] C. Mewes and T. Mewes, *Relaxation in Magnetic Materials for Spintronics, in: Handbook of Nanomagnetism* (Pan Stanford, 2015) p. 74.
[19] R. D. McMichael, D. J. Twisselmann, and A. Kunz, Phys. Rev. Lett. **90**, 227601 (2003).
[20] Y. Kasatani, S. Yamada, H. Itoh, M. Miyao, K. Hamaya, and Y. Nozaki, Applied Physics Express **7**, 123001 (2014).
[21] G. M. Müller, J. Walowski, M. Djordjevic, and G. X. Miao, Nature Materials **8**, 56 (2009).
[22] H. Lee, Y. Wang, C. Mewes, and W. H. Butler, Applied Physics Letters **95**, 082502 (2009).
[23] P. Landeros, R. E. Arias, and D. L. Mills, Physical Review B **77**, 214405 (2008).
[24] M. J. Hurben and C. E. Patton, Journal of Applied Physics **83**, 4344 (1998).
[25] R. D. McMichael, M. D. Stiles, and P. J. Chen, Journal of Applied Physics **83**, 7037 (1998).
[26] M. Farle, Reports on Progress in Physics **61**, 755 (1998).
[27] B. Heinrich and J. Bland, eds., *Radio Frequency Techniques, in: Ultrathin Magnetic Structures II* (Springer, 1994) p. 195.
[28] I. Barsukov, P. Landeros, R. Meckenstock, J. Lindner, D. Spoddig, Z.-A. Li, B. Krumme, H. Wende, D. L. Mills, and M. Farle, Phys. Rev. B **85**, 014420 (2012).
[29] G. Woltersdorf and B. Heinrich, Physical Review B **69**, 184417 (2004).
[30] M. Hashimoto, J. Herfort, H. P. Schonherr, and K. H. Ploog, Applied Physics Letters **87**, 102506 (2005).